DALTON
FULL PAPER

Effect of surfactant and pH on the redox potential of microperoxidase 11 in aqueous micellar solutions

Diganta K. Das and Okhil K. Medhi *

Department of Chemistry, Gauhati University, Guwahati-781 014, India

The redox potential of heme undecapeptide from cytochrome c (microperoxidase 11) in aqueous sodium dodecyl sulfate (sds), hexadecyltrimethylammonium bromide, and Triton X-100 surfactant micelles varied from +2 mV at pH 3.0 to −222 mV at pH 9.0. The potentials at pH 7.0 were −114, −122, and −166 mV *vs*. the normal hydrogen electrode in the three surfactants. The nature of the axial ligands, spin state of iron, apolar nature of the local heme environment, and pH influence the potential in the micelles. Binding of histidine (HisH) of the peptide chain gave a negative shift of −60 mV, and deprotonation of co-ordinated HisH to histidinate gave a −100 mV shift of the potential in aqueous sds. At pH 5.0–6.0 the axial ligands to iron are H_2O and HisH; deprotonation of co-ordinated H_2O gave −65 mV shift of the potential. Interaction of hemin with surfactant gave a positive shift of the potential with respect to that in water. The diffusion coefficient of the undecapeptide (2.4×10^{-7} cm^2 s^{-1}) at pH 7.0 in the micelles is an order of magnitude smaller than that in water, indicating solubilisation of heme in surfactant solutions. The potential is strongly dependent on pH and is controlled by the uptake/release of protons at three sites: the unco-ordinated HisH of the peptide chain, the axially co-ordinated H_2O and HisH ligands. The pK_a values of these redox state-dependent ionisations in the iron(III) state are *ca*. 4.3, 6.3, and 8.3. The change in potential per unit change of pH ($\Delta E/\Delta$pH) was *ca*. −59 mV, which indicates proton-coupled electron transfer involving one electron and one proton.

The cytochromes are heme-containing electron-transfer proteins. They exhibit a large positive redox potential relative to model hemes in aqueous solutions; for example +260 mV in cytochrome c as compared to −200 mV in complexes of natural hemes.[1,2] The redox potentials of cytochromes are determined by several factors such as the type of axial ligands,[3] nature of the environment (hydrophobicity) surrounding the heme,[1,2] hydrogen bonding by axial histidines[4,5] and the effect of the pH of the medium. A conformational change that results in the co-ordination of histidine to iron(II) in peroxidase imparts a pH dependence to the redox potential.[6] Recent structural studies on cytochrome c indicate the influence of the local heme environment[7] and hydrogen-bonding network on the reduction potential.[8] The pH-dependent potential of a mutant cytochrome c peroxidase is assigned to a high-spin to low-spin crossover[9] associated with deprotonation of axial ligands.[6] The redox potentials of several other cytochromes is controlled by proton equilibria of ionisable functional groups;[1,10,11] here the uptake of an electron at one centre is coupled to the uptake of a proton at another.[1] However experimental evidence in model systems in order to evaluate the influence of some of these factors on the redox potential is lacking.

The heme undecapeptide (microperoxidase 11) is a good model to study the electrochemical behaviour of heme iron in hemoproteins.[12–14] Rapid reversible electron transfer at a glassy carbon electrode is achieved even in the absence of a mediator or promoter.[14] The undecapeptide has peroxidase activity[15] (hence called microperoxidase) and presumably mimics cytochrome c peroxidase.[16] Obtained from enzymatic hydrolysis[12] of cytochrome c, the structure of microperoxidase includes protoporphyrin IX (3,7,12,17-tetramethyl-8,13-divinlyporphyrin-2,18-dipropanoic acid) covalently bonded by thioether bridges to Cys-14 and -17 residues of the native[17] horse heart cytochrome c ($L^1 = H_2O$ or imidazole of histidine of the peptide chain, $L^2 = H_2O$ or OH^-).

In ordinary aqueous solutions the amino group of valine-11 or lysine-13 of one molecule co-ordinated to iron of another leading to dimerisation or polymerisation of the undecapeptide.[17] Microperoxidase has low solubility at low pH and undergoes extensive aggregation in alkaline solution even in millimolar concentrations.[17,18] This makes a pH-dependence study of the spectroscopic and electrochemical behaviour of microperoxidase very problematic. However, the undecapeptide can be solubilised in aqueous sodium dodecyl sulfate (sds) micelles over a wide range of pH (1.8–10.0).[19] Encapsulation in micelles prevents intermolecular co-ordination and the heme monomers are present with a radial alignment[20] of the porphyrin near the micelle–water interface. The immediate microenvironment of hemes in aqueous micelles is predominantly apolar and the hydrophobic interactions of the heme with surfactants are found to be important to an understanding of interactions of the more complex hemoproteins.[20–22]

The proton NMR and optical spectra of microperoxidase 11 are markedly dependent on pH and show equilibrium conversion of various axially ligated species and a high- to low-spin crossover in aqueous sds.[19] Thus, in aqueous surfactant solutions the heme undecapeptide provides an opportunity to study the effect of axial ligands, apolar nature of the local heme environment, spin crossover, and proton equilibria on the redox potential of the heme group over a wide range of pH.

An area of current research interest is the electrochemical study of hemes and related systems in surfactant solutions or films.[23,24] In this paper we report the effect of three different surfactants on the midpoint potential of heme undecapeptide complexes. The proton equilibria and the dependence of the midpoint potential on pH are also reported.

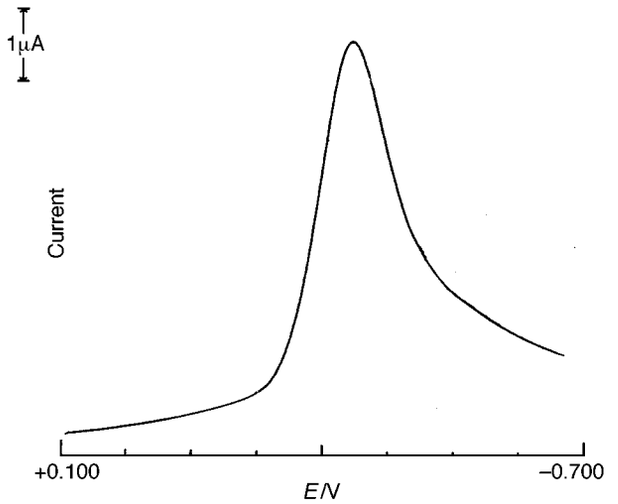

Fig. 1 Osteryoung square-wave voltammogram of microperoxidase 11 (0.5 mg cm^{-3}) in 4% aqueous sds micellar solution (glassy carbon electrode, Ag–AgCl reference, pH 7.0, 0.05 M Tris buffer)

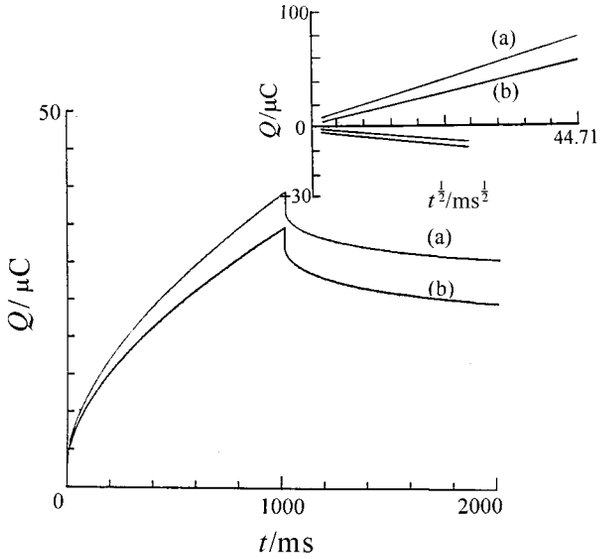

Fig. 2 Charge (Q) *versus* time response of chronocoulogram of microperoxidase 11 (0.5 mg cm^{-3}) in water (a) and 4% sds aqueous micellar solution (b). Inset: the Anson plot (Q *versus* $t^{\frac{1}{2}}$) for microperoxidase 11 in water (a) and 4% aqueous sds (b)

Experimental

Microperoxidase 11 and Triton X-100 were from Sigma Chemicals Co. USA, Sodium dodecyl sulfate, hexadecyltrimethylammonium bromide, tris(hydroxymethyl)aminomethane (tris buffer) and tetramethylammonium bromide from Merck BDH, UK. Sodium nitrate was recrystallised from doubly distilled water. The microperoxidase 11 and Triton X-100 were used without further purification, sds was recrystallised twice from ethanol–water mixture and $NMe_3(C_{16}H_{33})Br$ was purified by recrystallisation from acetone. Solutions of microperoxidase 11 in various surfactant micelles were prepared by following the reported procedure.[19] A slightly alkaline solution of microperoxidase 11 was added to a 4% aqueous surfactant solution and the mixture allowed to equilibrate in the dark at 40–50 °C for 1 h. The micellar solutions also contain 0.1 M NMe_4Br, and 0.1 M $NaNO_3$ as supporting electrolyte. The pH was adjusted using appropriate buffers (0.1 M) and measured as described previously.[19,21] The final concentration of the heme was *ca.* 10^{-5} M for optical spectroscopy and *ca.* 1 mM for electrochemical studies. The ionic strength was maintained at 0.2 M. Optical spectra were recorded on a Hitachi (model 3210) spectrophotometer. Solutions prepared in this way obeyed Beer's law over a wide range of concentration of microperoxidase 11. Surfactant solutions of varying concentrations were prepared by diluting a 4% stock solution of the surfactant. A slightly alkaline solution of microperoxidase was added to each of the solutions and the mixture equilibrated in the dark at 40–50 °C for about 1 h.

Electrochemical measurements were performed on a BAS 100B electrochemical analyser (Bioanalytical systems, USA) using a three-electrode assembly with nitrogen-gas purging lines. A glassy carbon disc was used as working electrode and Ag–AgCl (3 M aqueous NaCl) electrode was used as a reference; the standard potential of this electrode was taken[10] as +198 mV *versus* the normal hydrogen electrode. This working electrode was cleaned by polishing with a 0.1 μm alumina using a polishing kit (BAS) followed by sonication in a ultrasonicating bath. The potential of the reference electrode was periodically checked. The voltammograms were plotted on a Fujitsu FPG-300 plotter.

Background voltammograms of the surfactant solutions (containing 0.1 M NMe_4Br and 0.1 M $NaNO_3$) at a glassy carbon electrode showed the micelles were free from redox interferences in the potential range of interest.[25] All the measurements of the pH dependence of the midpoint potential were performed by Osteryoung square-wave voltammetry (OSWV). The square-wave amplitude was 25 mV, the frequency 15 Hz and the potential step height for the base staircase waveform was 4 mV. A typical square-wave voltammogram of microperoxidase 11 in aqueous micelles is shown in Fig. 1. The diffusion coefficient and the adsorption at the electrode surface was measured from the slope and intercept, respectively, of a plot of the charge (Q) *versus* the square root of time ($t^{\frac{1}{2}}$) for chronocoulometry data.[26,27] The chronocoulogram of heme undecapeptide in aqueous sds micelles is shown in Fig. 2.

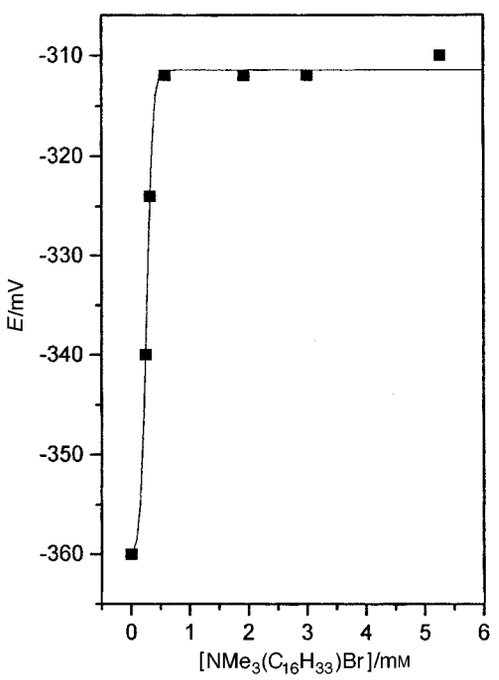

Fig. 3 Change of midpoint potential with $NMe_3(C_{16}H_{33})Br$ concentration (0.5 mg cm^{-3} microperoxidase 11 at pH 7.0, 0.05 M Tris buffer)

Results and Discussion

Effect of surfactant on the midpoint potential

The variation of the midpoint potential of heme undecapeptide with the concentration of surfactant is shown in Fig. 3. Gradual addition of surfactant to an aqueous solution of undecapeptide gave a positive shift which continued to increase until a surfactant concentration close to the critical micellar

Table 1 Midpoint potential (E_m), electronic spectra (λ_{max}), heme methyl proton NMR spectra, and solution magnetic moments (μ_{eff}) of microperoxidase 11 in aqueous surfactant solutions at 298 K

	E_m/mV						
pH	sds	Triton X-100	$NMe_3(C_{16}H_{33})Br$	λ_{max}/nm (sds)	^{1}H NMR/(δ) (sds)	μ_{eff}/μ_B (sds)	Ligation (L^1,L^2) and spin state
3.0	+2	−18	−2	396, 501, 530 (sh), 640	80–62	5.6	H_2O, H_2O; high
5.0	−57	−118	−33	398, 521, 555 (sh), 640	80–62	5.6	HisH, H_2O; high
7.0	−122	−166	−114	407, 528, 570 (sh)	30–10	2.3	HisH, OH^-; low
9.0	−222	−198	−195	409, 537, 570 (sh)	21–16	2.1	His^-, OH^-; low

Surfactant concentration 4%, E_m values *versus* the normal hydrogen electrode within ±5 mV, NMR and μ_{eff} values taken from ref. 19; $\mu_B = 9.27 \times 10^{-24}$ J T^{-1}

concentration (c.m.c.) was obtained. Above the c.m.c. the midpoint potentials are relatively unaffected;† the largest anodic shift was *ca.* +50 mV with respect to water (Fig. 3). Thus bringing an undecapeptide complex from an essentially aqueous environment to an essentially hydrophobic environment of micelles at pH 7.0 gave a positive shift of potential. The limiting values of potential at 4% aqueous surfactant, which is much above the c.m.c., are −114 ± 5, −122 ± 5, and −166 ± 5 mV (*versus* the normal hydrogen electrode at pH 7.0) in 4% aqueous $NMe_3(C_{16}H_{33})Br$, sds, and Triton X-100, respectively.

Double potential-step chronocoulometry showed that in aqueous sds and $NMe_3(C_{16}H_{33})Br$ solutions the charge (Q) *versus* time (t) response was typical of a diffusion-controlled process.[26,27] The response for the reverse step was linear and gave an intercept (background corrected) of 0.6 μC in aqueous surfactant as compared to that of 2.7 μC in water. The results indicate[26] that the reduction product of heme undecapeptide in aqueous surfactant solutions was weakly adsorbed at the electrode surface as compared to that in water. Thus the reduction processes in the surfactant solutions were less complicated by adsorption at the electrode surface.

The diffusion coefficients of heme undecapeptide in aqueous surfactant solutions at pH 7.0 are 2.4×10^{-7} and 1.3×10^{-7} cm^2 s^{-1} in aqueous sds and $NMe_3(C_{16}H_{33})Br$, respectively. These values are an order of magnitude smaller than that in water (2×10^{-6} cm^2 s^{-1}),[14] indicating that the undecapeptide is solubilised in surfactant micelles and diffuses to the electrode more slowly than in water. The slow rate of diffusion may be due to an increase in the effective size of micelle-encapsulated hemes and the high viscosity of the surfactant solutions.[26,29]

Effect of axial ligation on midpoint potential

The optical spectra, solution magnetic moments, and NMR spectra of heme undecapeptide in aqueous micellar solutions indicate the presence of H_2O, HisH, OH, and histidinate (His^-) as axial ligands to iron(III) under varying conditions[19] (Table 1). The midpoint potentials of the heme undecapeptide in 4% surfactant solutions, with different sets of axial ligands, are also given. A surfactant concentration much above the c.m.c. was chosen so that the midpoint potentials and the spectra are independent of any minor fluctuation in surfactant concentration.

Replacement of an aqua ligand by histidine of the peptide chain gave a negative shift of *ca.* −60 mV, and −30 mV in sds and $NMe_3(C_{11}H_{33})Br$, respectively (Table 1). Deprotonation of the co-ordinated water to a hydroxide gave a negative shift of the potential; −65 mV in sds and −81 mV in $NMe_3(C_{16}H_{33})Br$. Deprotonation of the co-ordinated HisH histidinate gave a very large negative shift of −100 mV in sds solution. The midpoint potentials in micellar solutions are larger and more positive than those of the undecapeptide in water with a similar set of axial ligands.[12–14]

Dependence of spectra and midpoint potential on pH

Fig. 4 shows the absorbance of heme at the Soret band as a function of pH in the range 3.0–10.0. Analysis of the results shows the existence of three acid–base equilibria with pK_a (i) at *ca.* 4.3, (ii) *ca.* 6.3, and (iii) *ca.* 8.3 in various surfactant solutions.‡ The NMR study in sds micelles[19] showed distinct changes of heme methyl proton signals at pH values near these pK_as. The pK_a values are dependent on the nature of the surfactant (Table 2). Based on the spectral data the probable ionisable groups associated with the pK_as are shown in Table 2.

The dependence of midpoint potential on pH in the range 4.0 to 6.0 is shown in Fig. 5(i). The potential remains relatively unchanged as the pH of the solution approaches the pK_a value (*ca.* 4.4); beyond this the potential shifts cathodically as the pH increases. The changes in potential per unit change in pH are −60 and −58 mV in sds and $NMe_3(C_{16}H_{33})Br$ micelles, respectively. The cathodic shift continues till the pH of the solution reaches 5.3 in sds and 5.1 in $NMe_3(C_{16}H_{33})Br$.

The spectral and magnetic properties of the undecapeptide at pH 3.0–5.0 (Table 1) indicate a typical six-co-ordinated high-spin complex; at pH 3.0 (<pK_a) the species present in solution is a diaqua hemin complex.[19] At pH 5.0 (>pK_a) the Soret band (398 nm) indicates binding of imidazole (HisH) to the hemin,[13] and α and β bands at 555 and 521 nm indicate a species similar to that of aqua metmyoglobin with HisH and H_2O as axial ligands.[19] Hence the transition with a pK_a of *ca.* 4.3 is due to binding of the peptide HisH to the heme, equation (3). The pK_a

$$HisH_2^+ + [FeL(H_2O)_2]^+ \rightleftharpoons [FeL(HisH)(H_2O)]^+ + H^+ + H_2O \quad (3)$$

value of the HisH binding equilibrium for the iron(II) undecapeptide was obtained by a weighted non-linear least-squares fit of the E_m *versus* pH data [Fig. 5(i)] to a theoretical curve[10,30] described by equation (4), where pK_r and pK_o are the pK_as of

$$E_m = E + \frac{RT}{nF} \ln \frac{K_r + [H^+]}{K_o + [H^+]} \quad (4)$$

† The reported[28,29] c.m.c. values at 25 °C are 4.0×10^{-4}, 9.2×10^{-4}, and 8.3×10^{-3} M in Triton X-100, $NMe_3(C_{16}H_{33})Br$, and sds, respectively. The value obtained from Fig. 3 was *ca.* 6×10^{-4} M for $NMe_3(C_{16}H_{33})Br$ which is acceptable considering the fact that c.m.c. values are sensitive to temperature and for ionic surfactants the values depend on the presence of electrolytes in solution.[28,29]

‡ The results were analysed by a weighted non-linear least-squares fit of the spectral data using the Henderson–Hasselbach equation (1) where

$$pK_a = m \cdot pH - \log([A^{m-}]/[H_mA]) \quad (1)$$

H_mA and A^{m-} are the acid and conjugate base, respectively, and m is the number of protons involved. The observed absorption coefficients,

$$H_mA = A^{m-} + mH^+ \quad (2)$$

ε_{obs}, can be written as $\varepsilon_0 - \alpha(\varepsilon_0 - \varepsilon_c)$, where $\alpha = K_a/(K_a + [H^+])$ is the fraction of the conjugate base complex and ε_0 and ε_c the extrapolated absorption coefficients of pure H_mA and A^{m-} species. In all the cases the best-fitted theoretical curve (Fig. 4) corresponds to one proton ionisation ($m \approx 1.0$). The pK_a values are obtained from the best-fitted curves.

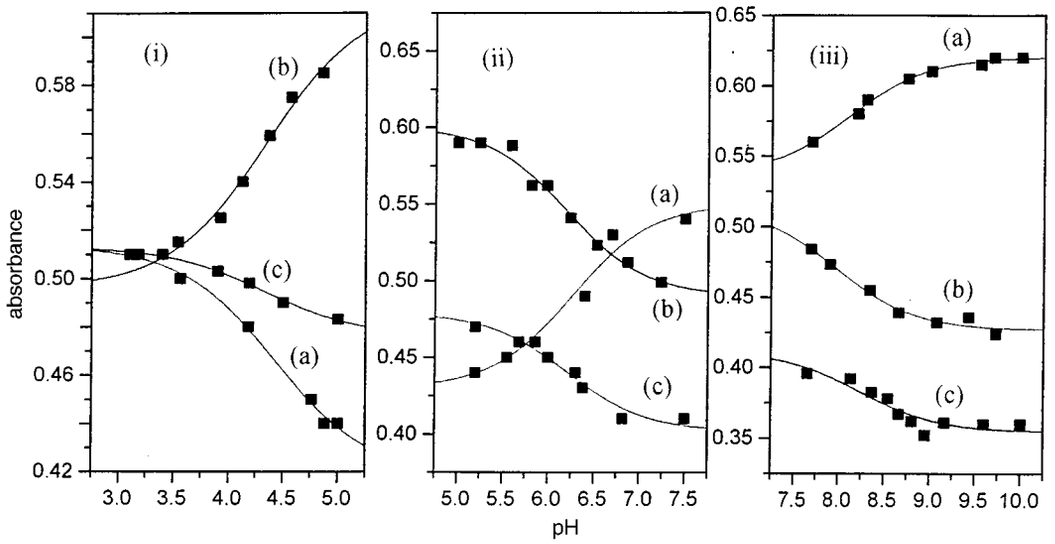

Fig. 4 Change in absorbance of the Soret band of microperoxidase 11 (*ca.* 10^{-5} M) in aqueous sds (a), $NMe_3(C_{16}H_{33})Br$ (b), and Triton X-100 (c) as a function of pH. The data in the pH range 3.0–10.0 are shown in three different segments corresponding to pK_a *ca.* 4.3 (i), *ca.* 6.3 (ii) and *ca.* 8.3 (iii)

Table 2 The pK_a values of iron(III) microperoxidase complexes in aqueous solutions of surfactants

pK_a			
sds	Triton X-100	$NMe_3(C_{16}H_{33})Br$	Possible ionisable group
4.3	4.4	4.3	Protonated histidine ($HisH_2^+$) of peptide chain
6.3	6.4	6.3	Co-ordinated H_2O
8.4	8.3	8.2	Co-ordinated HisH

The pK_as were measured from the pH dependence of the absorbance of the Soret band (Fig. 4) at 298 K and are within ±0.1.

Table 3 The pH dependence of the midpoint potential due to (i) histidine (of peptide) binding, (ii) aqua-hydroxo equilibrium, and (iii) ionisation of co-ordinated histidine

Medium	pK_o	pK_r	ΔpK_a	$(\Delta E_m/\Delta pH)$/mV
(i)				
sds	4.3	5.3	1.0	−60
$NMe_3(C_{16}H_{33})Br$	4.4	5.1	0.7	−58
(ii)				
sds	6.3	7.1	0.8	−59
$NMe_3(C_{16}H_{33})Br$	6.4	7.3	0.9	−57
(iii)				
sds	8.5	9.3	0.8	−58
$NMe_3(C_{16}H_{33})Br$	8.3	9.3	1.0	−57

The pK_o and pK_r values are the pK_as of the iron-(III) (oxidised) and -(II) (reduced) form of heme undecapeptide. They were obtained from least-squares fits of E_m *versus* pH data using equation (4); $\Delta pK_a = pK_r - pK_o$.

the proton equilibria in the iron(II) and the -(III) state of the heme undecapeptide. The pK_r and pK_o values in various surfactant solutions are given in Table 3. The change in potential per unit change in pH ($\Delta E/\Delta pH$) of *ca.* −59 mV indicates that one proton and one electron was transferred.

The dependence of midpoint potential on pH in the range 6.0 to 8.0 shows that the potential shifts cathodically as the pH increases [Fig. 5(ii)], implying that the reduction is accompanied by proton equilibria.[10] The result was analysed by a weighted non-linear least-squares fit of the potential using a theoretical curve[10,30] described by equation (4). The best-fitted theoretical curve corresponds to one electron ($n \approx 1$) and one proton ionisation. The pK_a values obtained from the curve-fitting procedure are given in Table 3. The spectral data and the solution magnetic behaviour[31] of the undecapeptide at pH 6.0–7.0 indicate the existence of a high- to low-spin crossover of iron(III) with a pK_a *ca.* 6.3. At pH 6.0 the species present is high-spin $[FeL(HisH)(H_2O)]^+$, while at pH 7.0 the spectrum of the low-spin complex[19] (Table 1) is similar to that of a hemin with an imidazole and a hydroxide as the axial ligands.[32] Hence the transition with a pK_a *ca.* 6.3 is due to an aqua–hydroxo equilibrium (5). The pH dependence of the potential was analysed

$$[FeL(HisH)(H_2O)]^+ \rightleftharpoons [FeL(HisH)(OH)] + H^+ \quad (5)$$

in terms of a pK_{o1} of *ca.* 6.3 in the iron(III) form and pK_r *ca.* 7.3 in the iron(II) form of the undecapeptide (Table 3). The pK_{o1} values agree well with that found[19] from optical spectroscopy§ (Table 2) and that reported[31] in sds by solution magnetic moment measurement. The pK_o value of an axial ligand is essentially due to the polarising effect of the metal; reduction of iron(III) raises the pK_r value of that ligand in the iron(II) complex. At pH values above pK_o the iron(III) complex is [FeL(HisH)(OH)] and below pK_r the iron(II) complex is $[FeL(HisH)(H_2O)]$; reduction in the pH range $pK_o < pH < pK_r$ takes place with an uptake of a proton. The change in potential per unit change in pH, $\Delta E/\Delta pH$, *ca.* −59 mV (Table 3) indicate involvement of one proton and one electron according to equation (6).

$$[FeL(HisH)(OH)] + e^- + H^+ \rightleftharpoons [FeL(HisH)(H_2O)] \quad (6)$$

Above pH 8.0 there are further cathodic shifts of the potential [Fig. 5(iii)] with pK_o at 8.3 and 8.5 in $NMe_3(C_{16}H_{33})Br$ and sds solutions, respectively (Table 3). The pK_a values calculated from the electrochemistry data are in agreement with those obtained from spectroscopy. The optical spectra at high pH (9.0–10.0), with the α and β bands at 570 and 537 nm, were similar to that of a hemin complex with a deprotonated imidazole and a hydroxide ion as the axial ligands.[32] For an analogous complex of heme octapeptide in methanol–water solution, with a histidinate (imidazolate) and a hydroxide ion as axial ligands to iron, the α and β bands were found at 565 and 535 nm, respectively.[33] The NMR spectrum[19] indicates a low-spin

§ In an earlier report[19] the pH dependence of absorbance (at 408 nm) data was fitted by a single pK_a at 7.2. The same data can be fitted by two pK_as at 6.3 and *ca.* 8.3.

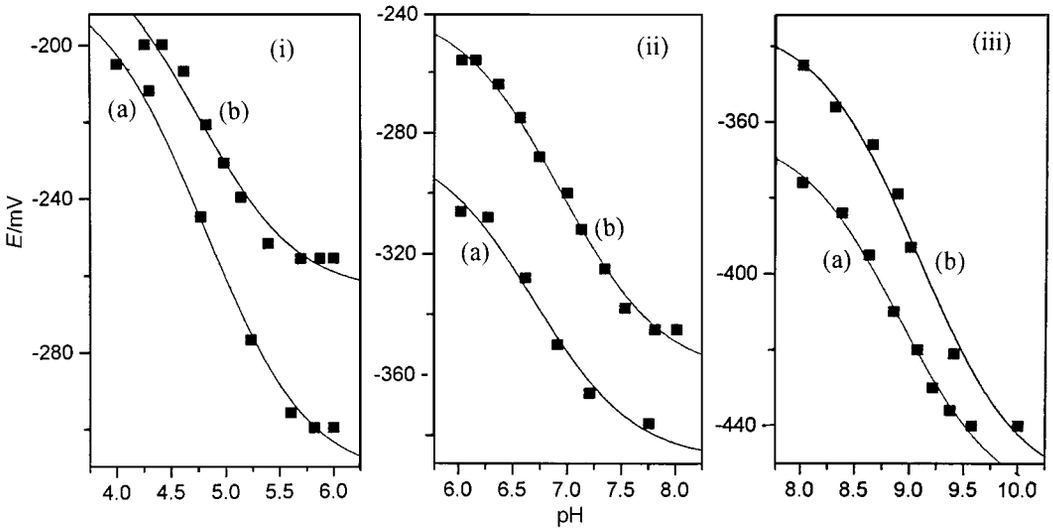

Fig. 5 The pH dependence of the midpoint potential of microperoxidase 11 (0.5 mg cm^{-3}) encapsulated in aqueous sds (a) and $NMe_3(C_{16}H_{33})Br$ (b) in three segments: (i) from pH 4.0 to 6.0, (ii) from pH 6.0 to 8.0 and (iii) from pH 8.0 to 10.0. The potentials were measured by OSWV on a glassy carbon electrode *vs.* Ag–AgCl, $I = 0.1$ M $NaNO_3$

form different from that of the hydroxo complex at pH 7.0 (Table 1). In aqueous solutions at high pH imidazole probably binds to the undecapeptide in the deprotonated form.[17] Thus the proton equilibrium with a pK_a *ca.* 8.3 is due to the ionisation of co-ordinated histidine, equation (7). Deprotonation of

$$[FeL(HisH)(OH)] \rightleftharpoons [FeL(His)(OH)]^- + H^+ \quad (7)$$

co-ordinated imidazole to an imidazolate would increase the electron density at the metal,[34,35] making the reduction of iron(III) more difficult, and the midpoint potential shifts to more negative values[4,5] as the pH increases [Fig. 5(iii)].

For the analogous monomeric heme octapeptide in 20% (v/v) methanol–water[33] the three ionisations [equations (3), (5) and (7)] were found with pK_a values at 4.43, 8.9, and 10.48. The lower pK_a values of co-ordinated ligands in the micelles (Table 2) may be due to the hydrophobic effect of surfactants;[21,22] for example, the pK_a of co-ordinated water in diaqua hemin[21] was lowered from 7.5 in water to 5.5 in sds micelles and that in an aqua(pyridine) hemin complex[36] was lowered from 10.5 in water to 7.7 in aqueous $NMe_3(C_{16}H_{33})Br$.

Comparison with proteins

A change in the local heme environment on bringing the undecapeptide from an aqueous solution to an essentially hydrophobic environment at the micelle–water interface gave a positive shift of the midpoint potential. This supports the hypothesis[1,2] that a hydrophobic local heme environment of a apoprotein could give a large positive redox potential for cytochromes. However, the effective relative permittivity of the local heme environment of the micelle–water interface ($\varepsilon = 32$)[37] is much larger than that in proteins.[2] Therefore, the positive shift of potential in micelles with respect to water was not as large as those found for the cytochromes.[2] Moreover, other factors such as the pH of the medium, iron spin states, and the nature of the axial ligands play an important role in influencing the redox potentials.

The pH dependence of the redox potential due to deprotonation of an unco-ordinated $HisH_2^+$ residue of the peptide chain in close proximity to heme as in[10] cytochrome c_2 and probably in cytochrome c peroxidase[6] was demonstrated for the undecapeptide in aqueous surfactants. The presence of a positively charged $HisH_2^+$ close to iron of heme (at low pH) would tend to destabilise the iron(III) complexes with respect to the iron(II) complexes [due to electrostatic interaction with the net positive charge on iron(III)[10] causing the midpoint potential to fall with increasing pH].

A pH-induced high- to low-spin crossover as in the Asp-235 mutant[9] of cytochrome c peroxidase (ccp), which was associated with an aqua–hydroxo equilibrium,[6] was also found in aqueous surfactant solutions of the undecapeptide. In the ccp mutants there was a further transition to a second low-spin species[6,9] by binding another histidine;[6] the structural changes suggested for this were different from that found in the heme undecapeptide. The redox potentials of other peroxidases also exhibit two breaks in the E_m *vs.* pH curve.[9]

As in the cyano complex of horseradish peroxidase;[38] the undecapeptide contains a histidinate anion as axial ligand to iron(III) in alkaline solutions. The proposal that HisH ionisation depends on the redox state of iron in the peroxidases[4,5] was demonstrated for the undecapeptide. In several hemoproteins the pK_a of histidine ionisation is in the range 7–9; the exact value depends on the nature of the heme environment and on the presence of Lys or Arg residues near the heme.[11] Similar effects may be responsible for the low pK_a of histidine ionisation in the undecapeptide; the hydrophobic effect of micelles[21,22] and the positively charged side chains of Lys in the peptide can provide substantial stabilisation of the histidinate anions by salt-link formation.[11]

Conclusion

Aqueous surfactant solutions not only solubilise and stabilise monomeric iron(II) and -(III) forms of heme undecapeptide but also allow spectroscopic and electrochemical study over a wide range of pH. In an aqueous surfactant solution of the undecapeptide the midpoint potentials are more positive with respect to that in water; the largest positive shift was found in cationic surfactant. The behaviour is attributed to the influence of solubilisation and stabilisation of the iron(II) hemes by the apolar nature of the local heme environment at the water–micelle interface. The potential is further influenced by binding of axial ligands (HisH of peptide chain and H_2O), and their subsequent deprotonation. A high- to low-spin crossover near pH 7.0 also controls the midpoint potentials.

Electron transfer in the undecapeptide in aqueous micellar solutions (pH 4.0–10.0) was controlled by the uptake/release of protons at three sites: the imino-nitrogen atom of unco-ordinated imidazole of histidine, the axially co-ordinated H_2O/OH ligand, and the co-ordinated histidine of the peptide chain. The pK_as of these ionisations are widely separated between the

iron-(III) and the -(II) oxidation state in the heme. The midpoint potential of heme undecapeptide was found to be strongly dependent on the state of protonation of the axial ligands; proton uptake at the axial ligands can therefore control the redox potential of the heme. Thus the heme undecapeptide in aqueous surfactant solutions was found to be good model to study how the proton uptake at several ionising groups influences the redox potential of heme proteins.

Acknowledgements

The authors acknowledge the University Grants Commission, New Delhi for grants under the Special Assistance Programme. D. K. D. thanks the Council of Scientific and Industrial Research, New Delhi for grants of a research fellowship. We also thank Dr. E. D. Jemmis, Professor in Chemistry, Hyderabad Central University for his help in the curve-fitting procedures.

References

1 G. R. Moore and G. W. Pettigrew, *Cytochrome c: Evolutionary, Structural and Physiochemical Aspects*, Springer, Berlin, Heidelberg, 1990, ch. 7, pp. 309–362.
2 R. J. Kassner, *J. Am. Chem. Soc.*, 1973, **95**, 2674.
3 T. Mashiko, C. A. Reed, K. J. Haller, M. E. Kassener and W. R. Scheidt, *J. Am. Chem. Soc.*, 1981, **103**, 5758.
4 P. O'Brien and D. A. Sweigart, *Inorg. Chem.*, 1985, **24**, 1405.
5 R. Quinn, J. Mercer-Smith, J. N. Burnstyn and J. S. Valentine, *J. Am. Chem. Soc.*, 1984, **106**, 4136.
6 G. Smulevich, M. A. Miller, J. Kraut and T. G. Spiro, *Biochemistry*, 1991, **30**, 9546.
7 A. M. Berghuis, J. G. Guillemette, G. McLendon, F. Sherman, M. Smith and G. D. Brayer, *J. Mol. Biol.*, 1994, **236**, 786.
8 A. M. Berghuis, J. G. Guillemette, M. Smith and G. D. Brayer, *J. Mol. Biol.*, 1994, **235**, 1326.
9 D. B. Goodwin and D. E. McRee, *Biochemistry*, 1993, **32**, 3313.
10 G. R. Moore, D. E. Harris, F. A. Leitch and G. W. Pettigrew, *Biochim. Biophys. Acta*, 1984, **764**, 331.
11 G. R. Moore, R. J. P. Williams, J. Peterson, A. J. Thomson and F. S. Mathews, *Biochim. Biophys. Acta*, 1985, **829**, 83.
12 H. A. Harbury and P. A. Loach, *J. Biol. Chem.*, 1960, **235**, 3640.
13 H. A. Harbury and P. A. Loach, *Proc. Natl. Acad. Sci. USA*, 1959, **45**, 1344.
14 R. Santucci, H. Reinhard and M. Brunori, *J. Am. Chem. Soc.*, 1988, **110**, 8536.
15 N. J. Feder, *Histochem Cytochem.*, 1970, **18**, 911.
16 J. E. Erman and J. D. Satterlee, *Electron Transport and Oxygen Utilisations*, ed. C. Ho, Elsevier-North Holland, Amsterdam, 1982, pp. 223–227.
17 M. T. Wilson, R. J. Ranson, P. Masiakowski, E. Czarneka and M. Brunori, *Eur. J. Biochem.*, 1977, **97**, 193.
18 K. Kimura, J. Peterson, M. Wilson, D. J. Cookson and R. J. P. Williams, *J. Inorg. Biochem.*, 1981, **15**, 11.
19 S. Mazumdar, O. K. Medhi and S. Mitra, *Inorg. Chem.*, 1991, **30**, 700.
20 J. Simplicio, K. Schewenzer and F. Maenpa, *J. Am. Chem. Soc.*, 1975, **97**, 7319.
21 J. Simplicio, *Biochemistry*, 1972, **11**, 2525; J. Simplicio and K. Schewenzer, *Biochemistry*, 1973, **12**, 1923.
22 J. H. Fendler and E. J. Fendler, *Catalysis in Micellar and Macromolecular Systems*, Academic Press, New York, 1975, ch. 13, pp. 249 and 250.
23 J. F. Rusling, *J. Am. Chem. Soc.*, 1993, **115**, 11 891.
24 J. F. Rusling, N. Hu, H. Zhang, D. Howe, C.-L. Miaw and E. Coulter, *Electrochemistry in Colloidal Dispersions*, ed. R. A. Mackay and J. Texter, VCH, New York, 1992, pp. 303–318.
25 J. R. Kirchoff, E. Deutsch and W. R. Heinman, *Anal. Lett.*, 1989, **22**, 1323.
26 J. R. Kirchoff, W. R. Heinman and E. Deutsch, *Inorg. Chem.*, 1988, **27**, 3608.
27 A. J. Bard and L. R. Faulkner, *Electrochemical Methods, Fundamentals and Applications*, Wiley, New York, 1980, ch. 12, p. 535.
28 J. H. Fendler and E. J. Fendler, *Catalysis in Micellar and Macromolecular Systems*, Academic Press, New York, 1975, ch. 2, p. 20.
29 B. Lindman and H. Wennerstrom, *Top. Curr. Chem.*, 1980, **87**, 1.
30 W. M. Clark, *Oxidation Reduction Potentials of Organic Systems*, Williams and Wilkins, Baltimore, MD, 1960, pp. 256–263.
31 A. M. T. Jehanli, D. A. Stotter and M. T. Wilson, *Eur. J. Biochem.*, 1976, **71**, 613.
32 T. Yoshimura and T. Ozaki, *Arch. Biochem. Biophys.*, 1984, **230**, 466.
33 D. A. Baldwin, H. M. Marques and J. M. Pratt, *J. Inorg. Biochem.*, 1988, **27**, 245.
34 T. Mincey and T. G. Taylor, *J. Am. Chem. Soc.*, 1979, **101**, 765.
35 J. T. Landrum, K. Hatano, W. R. Scheidt and C. A. Reed, *J. Am. Chem. Soc.*, 1980, **102**, 6729.
36 S. Mazumdar, N. Kannadagulli, O. K. Medhi and S. Mitra, *J. Chem. Soc., Dalton Trans.*, 1989, 103.
37 M. S. Farnandez and P. Fromherz, *J. Phys. Chem.*, 1977, **81**, 1755.
38 J. S. de Ropp, V. Thanabal and G. N. LaMar, *J. Am. Chem. Soc.*, 1985, **107**, 8268.

Received 4*th December* 1997; *Paper* 7/08732B